Formation of Gold Bone Nanorods shape using copper as foreign metal ion

Suratun Nafisah [a] *, Marlia Morsin [b,c] *, Nurul Alia Fatin Redzoan [c,d], Nur Liyana Razali [b,c], Natasya Salsabiila [a,b,c], and Ahmad Nasrull Mohamed [c]

[a]Department of Electrical Engineering, Faculty of Industrial and Production Technology, Institut Teknologi Sumatera, Lampung Selatan, 35365, Indonesia
[b]Microelectronics & Nanotechnology - Shamsuddin Research Centre (MiNT-SRC), Institute of Integrated Engineering, Universiti Tun Hussein Onn Malaysia, 86400 Parit Raja, Batu Pahat Johor, Malaysia
[c]Department of Electronic Engineering, Faculty of Electrical and Electronic Engineering, Universiti Tun Hussein Onn Malaysia, 86400 Parit Raja, Batu Pahat Johor, Malaysia
[d]On Semiconductor Malaysia Sdn. Bhd. (Malaysia), Lot 122, Senawang Industrial Estate, 70450, Seremban, Negeri Sembilan, Malaysia
∗Corresponding author. e-mail: suratun.nafisah@el.itera.ac.id; marlia@uthm.edu.my

ABSTRACT

In this study, copper (Cu) is introduced as a foreign metal ion replacing platinum by modifying the recipe of GNBPs and the final structure obtained is gold bone nanorods (GBNRs). The aspect ratio and surface density of GBNRs were investigated by varying the growth time during the growth process from 30 minutes to 5 hours. It was found that the growth solution has been changed from colourless to light blue and violet colour with increasing growth time, indicating the formation of GBNRs. The UV-Vis analysis shows two resonance plasmon peaks for t-SPR and l-SPR at 583 nm and 766 nm with the intensity of 1.433 a.u and 2.236 a.u at the optimum 5 hours growth time. For morphological analysis, it was found that the sample with lower growth time produced gold nanosphere shapes and with increasing time, more GBNRs with large aspect ratios were produced. HR-TEM characterization reveals that bone nanorods are formed due to the influence of Cu foreign metal ions, which cause selective deposition of Au atoms onto {111} facet of gold nanorods, while simultaneously reducing the overgrowth rate of the {110} facet for the edge regions and the {100} facet for the tip regions of the nanorods. In addition, the influence of Cu foreign metal ions on the growth mechanism of Au nanoseeds into nanorods and the shape transformation of nanorods into bone nanorods are also discussed in this work. In conclusion, the GBNRs have been successfully synthesized using SMGM by induced Cu as foreign metal ions.

Keywords: Localized surface plasmon resonance, Gold bone nanorods, Gold nanorods, Seed mediated growth method, Growth time

1. INTRODUCTION

There are various types of metal nanoparticles such as gold (Au) [1], [2], silver (Ag) [3], [4], and copper (Cu) [5] used in sensing applications. These metals have unique characteristics namely Localized Surface Plasmon Resonance (LPSR) resulting from the collective oscillation of electrons on the metal nanoparticles by the interaction of the incident light and electrons at the resonant frequency. It will produce strong peaks in extinction spectra, as well as strong enhancements of the local electromagnetic fields surrounding the nanoparticles [6], [7]. The commonly used metal nanoparticle is gold due to its inert and chemical stability [8], [9].

Currently, gold with non–spherical structures has been chosen to be implemented in LSPR sensors [10]-[13]. These elongated structures have two LPSR plasmonic peak responses associated with transverse surface plasmon resonance (t-SPR) and longitudinal surface plasmonic resonance (l-SPR). The l-SPR response gives additional sensing parameters compared to spherical-based LSPR sensors [14], [15].

Gold nanorods (GNRs) and gold nanobipyramids (GNBPs) are fabricated elongated nanostructures that exhibit two LSPR plasmonic bands and have been used in LSPR sensing applications [16], [17]. These elongated nanoparticles are usually fabricated using the most popular gold nanoparticle synthesis method, namely the seed-mediated growth method (SMGM). By varying the growth parameters, such as materials and concentrations, rods and bipyramids can be produced. One of the most crucial ingredients for synthesizing elongated nanoparticles using SMGM is foreign metal ions, which play a role as a shaping agent to tune the morphology of nanoparticles. For example, GNRs can be obtained by modifying foreign metal ions using silver [18], [19]. In contrast, GNBPs are modified using platinum [20] as the foreign metal ion to form its shape during synthesis.

Thus, in this study, copper (Cu) is introduced as a foreign metal ion by modifying the recipe of GNBPs. As known, Cu is cheaper than platinum and silver. Even though Cu is more easily oxidized and corroded, the introduction of Cu as a foreign metal ion will not affect the properties of the gold

nanoparticles since the number of Cu atoms is very small compared to the number of gold atoms. The final structure obtained is GNRs with a bone shape called gold bone nanorods (GBNRs). The properties of GBNRs have been studied by varying their growth time. The bone shape nanorods produce two peaks of plasmonic response and are good to be used as sensing materials as an alternative to elongated nanoparticles, i.e., nanorods.

2. EXPERIMENTAL

The recipe of GBNRs used in this process was modified from the GNBPs recipe as previously reported [21], [22]. The synthesis of GBNRs was carried out utilizing the SMGM, which comprises two primary phases: seeding and growth. In the seeding phase, nanoseeds are implanted, while in the growth phase, the nanoseeds are nurtured to reach the desired shape and size over a specified growth period. The chemicals employed in this synthesis procedure included Gold (III) Chloride Trihydrate ($HAuCl_4$), Cyltrimethylammonium Bromide (CTAB), Sodium Borohydride ($NaBH_4$), and L-Ascorbic Acid (AA), all procured from from Sigma-Aldrich. Whereas Copper (II) Sulfate Pentahydrate (Cu) was purchased from Kanto Chemical Co. Inc., Silver nitrate ($AgNO_3$) was sourced from Honeywell, while Hydrochloric Acid (HCl) was acquired from ACI Labscan.

For the seeding process, four types of chemical materials are involved which are $HAuCl_4$, CTAB, $NaBH_4$, and Cu as the foreign metal ion. The process started by diluting the CTAB with deionized water for 9.75 ml. CTAB solution was immersed in the hot water to make it dilute and well mixed. The final CTAB solution is colourless. After that, 0.15 ml of $HAuCl_4$ was dropped into the CTAB solution. The colour turned from colourless to light gold. Then, 0.1 ml Cu was dropped into the seed solution. The colour remains the same. Lastly, icy cold $NaBH_4$ dropped into the solution and turned the light gold colour to a brownish colour. $NaBH_4$ needs to be stored in a cool place before being used to ensure this chemical is not affected by the constant changes in temperature and humidity. The seed solution was observed within 2 hours to see the colour changes. After 2 hours, the seed solution colour was changed from brownish to violet. Figures 1(a) and (b) show the seeding process for GBNRs.

After that, the growth process solution involved 7 types of chemical materials and a solution from the seeding process was prepared. The growth process started by diluting the CTAB with deionized water for 20 ml. After that, 0.875 ml of

$HAuCl_4$ was dropped into the CTAB solution. The colour turned from colourless to gold colour. Then, 0.025 ml Cu was dropped into the growth solutions. The colour still remains the same. Then, 0.2 ml of $AgNO_3$ was dropped followed by 0.4 ml of HCl. The colour of the solution remained the same for both processes. After that, 0.16 ml of AA was dropped and the colour changed from gold to colourless. This shows the reduction of gold chloride in the solution. Lastly, 0.05 ml of the seed solution was added and the solution was still colourless as shown in Figure 1(c). The duration of the growth process ranged from 30 minutes to 5 hours, with intervals of 1 hour, to investigate how the aspect ratio and surface density of the resulting GBNRs were affected by the growth time.

After that, the growth solution was undergoing the centrifugation process using Eppendorf Centrifuge 5804 (Germany). Centrifugation is a method that utilizes centrifugal force to segregate particles within a solution based on their size, shape, density, viscosity of the medium, and the speed of the rotor. Each sample needs to undergo 3 centrifugation processes in sequence which are 1 hour for 15 ml, 30 minutes for 3 ml and another 30 minutes for 3 ml. The growth solution has been centrifuged to separate the precipitate and supernatant. The precipitates can be seen at the bottom of the centrifuge tubes while the supernatant was removed using a pipette.

Finally, the optical characteristics of GBNRs were analyzed utilizing a UV-1800 Spectrophotometer manufactured by Shimadzu (Japan), operating within a range from 400 nm to 1000 nm. Morphological structures were examined through field-emission scanning electron microscopy (FESEM) using the JSM-7600F machine from Jeol (USA), under high vacuum conditions with a 5 kV accelerating voltage and high-resolution transmission electron microscopy (HR-TEM) using JEM-ARM200F machine from Jeol (USA). Structural analysis via X-ray diffraction (XRD) spectrum was conducted using the X'Pert Powder X-Ray Diffractometer produced by PANalytical (Netherlands), employing CuKα radiation with a wavelength of 1.5406 Å.

3. RESULTS AND ANALYSIS

The growth of GBNRs in the solution was accomplished. This was verified through four types of characterization: physical, optical, morphological, and structural analyses. The specific findings are elaborated as discussed below.

3.1. Physical Observation

The physical characterization can be observed by monitoring the colour changes in the seeding process and growth process. As previously mentioned, during the seed solution preparation, a mixture of CTAB solution and $HAuCl_4$ resulted in a light-yellow solution. Subsequently, Cu was introduced. Upon adding freshly prepared icy cold $NaBH_4$ to the seed solution, the solution's colour transitioned from light yellow to brownish, signifying the formation of nanoseeds within the solution as shown in Figure 1(a). After 2 hours, the seed solution turned from a brownish colour to a violet colour, as shown in Figure 1(b).
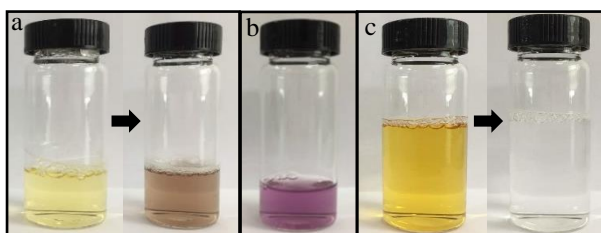

Figure 1. (a) Colour changes during the seeding process; (b) Final seed solution after 2 hours seeding period; (c) colour changes during the growth process

Then, the growth solution preparation started by mixing CTAB solution with HAuCl₄. The solution turned from colourless into gold colour. After that, Cu, AgNO₃ and HCl were added to the growth solution. For this process, the colour remains the same. The gold colour solution turned colourless as ascorbic acid was added to it. The colour changes are shown in Figure 1(c). Lastly, seed solution was added to the growth solution. The changes in the growth solution can be seen after 30 minutes from pale violet to light violet.

Figure 2(a) shows the result of the growth process with increasing growth time. After that, the solution was undergoing the centrifugation process. Figure 2(b) shows the variations of the growth solution after the centrifugation process. The solution after centrifuging shows a darker colour indicating a high density of particle formation.

3.2. Optical, Morphological, and Structural Properties of GBNR

The optical characterization was used to obtain the LSPR response of GBNRs from a UV-Vis spectrophotometer. For the growth process, the result was taken right after the growth process was completed within the set time. The absorption spectra of GBNRs were recorded with deionized water as references. Figure 3 shows the UV-Vis result of GBNRs before and after the centrifugation process with the variation of growth time.

From Figure 3, it can be seen that for 30 minutes to 1 hour, there is only a single t-SPR response with no l-SPR response. Then, the l-SPR peaks occurred after the growth time extended to 2 hours. After the growth time was extended to
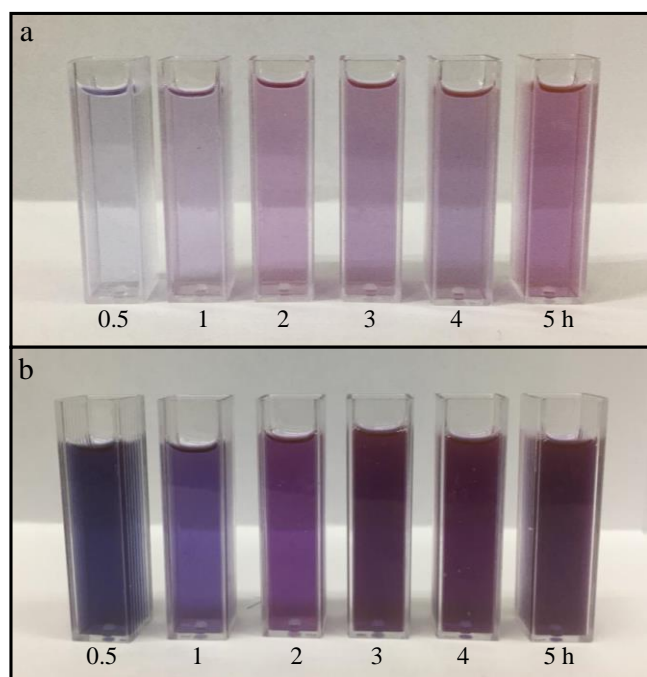
3-4 hours, clear and sharp peaks for both t-SPR and l-SPR response were obtained. For 5 hours of growth time, it has a stronger l-SPR response than t-SPR. The t-SPR refers to an oscillation of free electrons in a horizontal direction while l-SPR is obtained from the free charge in a vertical direction [23]. The detailed intensity and wavelength of the samples are listed in Table 1.
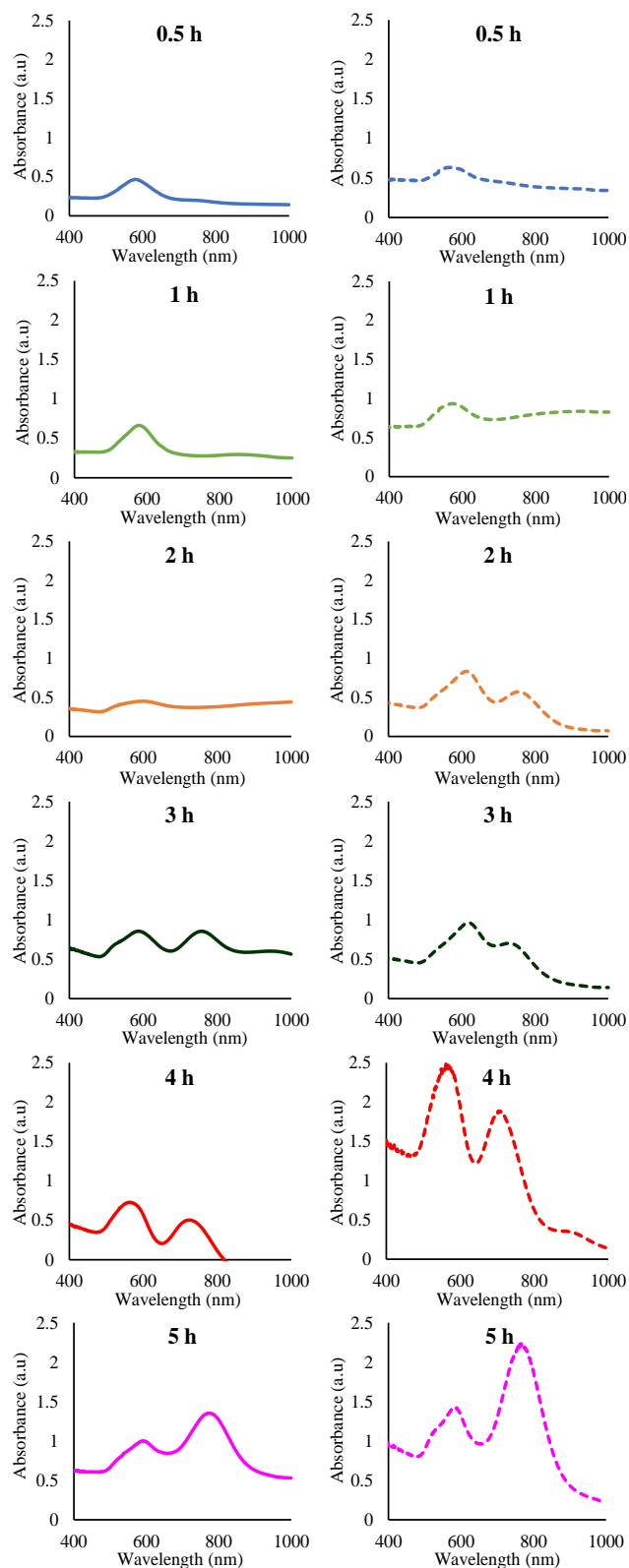

Figure 2. Growth solution with a variation of growth time from 0.5 to 5 hours (a) before centrifugation; (b) after the centrifugation process

Figure 3. UV-Vis spectrum of GBNRs before (solid line) and after (dashed line) centrifuged with a variation of growth time from 0.5 to 5 hours

Table 1. The detailed intensity and wavelength of the GBNRs

Growth Time (h)	Wavelength (nm)		Intensity (a.u.)	
	t-SPR	l-SPR	t-SPR	t-SPR
0.5	566	-	0.634	-
1	574	-	0.936	-
2	612	730	0.834	0.571
3	616	752	0.963	0.704
4	564	704	2.504	1.884
5	583	766	1.433	2.236

The LSPR response is related to the aspect ratio (width and length) of GBNRs. Single t-SPR response indicated very low formation of rods or only spherical particles formed within the growth period. GNRs usually exhibit two plasmon peaks at t-SPR and l-SPR [10], [12], whereas gold nanospheres exhibit only one plasmon peak [24]. Thus, the l-SPR gives an additional parameter that is potentially used in the LPSR sensor as a detection parameter.

Further analysis was done to confirm this finding using FESEM morphological images. For the morphological analysis, the magnification used for this analysis is 100k. Figure 4 shows the FESEM images of the GBNRs with variations in growth time.

As can be seen in the FESEM analysis, the sample for 30 minutes and 1 hour growth time has more spherical particles rather than rod particles. For 2 hours, more GBNRs were produced. 3 hours and 4 hours growth contain a high density of GBNRs. Whereas for sample 5 hours, the GBNRs produced have much bigger dimensions than other samples. The aspect ratio and surface density for all samples are listed in Table 2.

The aspect ratio was measured by the width and length of each GBNRs particle. According to this analysis, it can be seen that with the increasing of time, the aspect ratio of GBNRs also increases with the highest aspect ratio obtained for 5 hours of growth time which is 2.46 ± 0.06. Then, the surface density of GBNRs was measured using ImageJ software to calculate the number of particles per unit area of the surface. The higher the growth time produced a higher percentage of extracted GBNRs deposited on the surface of the substrate. Longer growth time with the same amount of gold source may cause stacking and overlapping of GBNRs which is not very good for LSPR sensors.

The HR-TEM images of GBNRs are shown in Figure 5. The low magnification, Figure 5(a), shows the perfect formation of bone nanorods. The observation of HR-TEM images

Table 2. Aspect ratio and density of the GBNRs

Growth time (h)	Aspect ratio	Surface density (%)
0.5	2.32 ± 0.05	14.58
1	2.33 ± 0.05	37.14
2	2.43 ± 0.06	38.58
3	2.44 ± 0.08	46.24
4	2.45 ± 0.05	54.06
5	2.46 ± 0.06	64.92
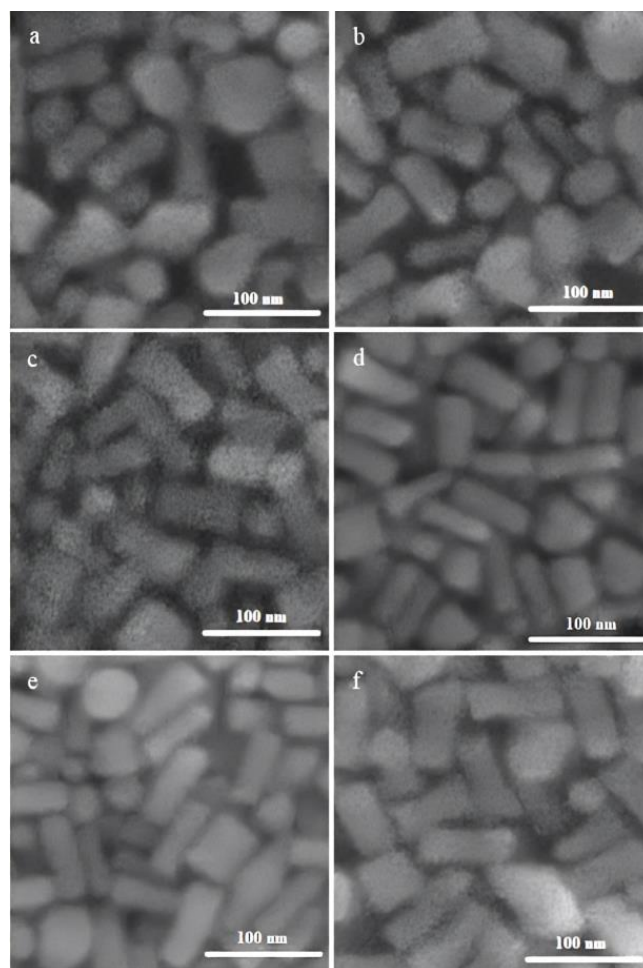
Figure 4. FESEM images of the GBNRs with variations of growth time (a) 0.5; (b) 1; (c) 2; (d) 3; (e) 4; (f) 5 hours
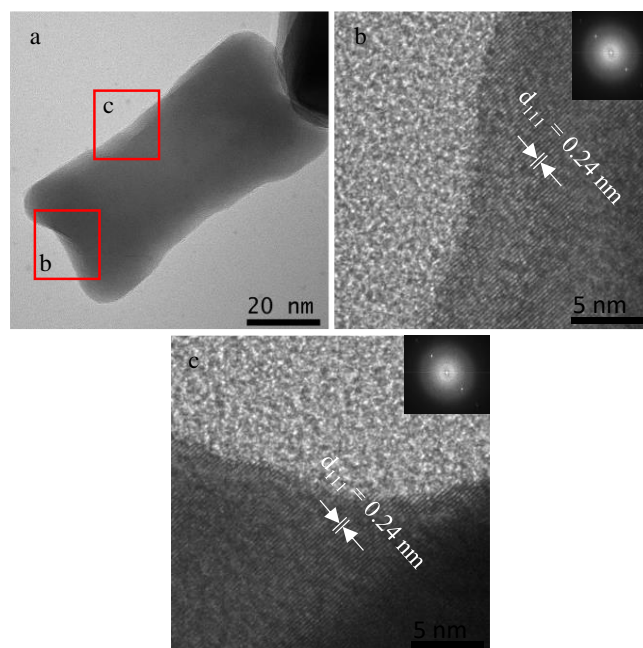
Figure 5. TEM images of GBNRs obtained at a growth time of 5 hours show (a) the perfect formation of bone nanorods; the area delineated by the square in (a) denotes the positions from which HR-TEM images in (b) and (c) were captured. Insets within (b) and (c) represent the fast Fourier transform (FFT) patterns corresponding to their respective images

indicates that bone nanorods emerge from nanorods with a diminished rate of overgrowth, particularly in the [100] direction for the tip regions and in the [110] direction for the edge regions as shown in Figure 5(b) and 5(c), respectively. The reduced overgrowth rate observed in the [100] direction at the tips and in the [110] direction at the edges implies a regulated growth process influenced by the presence of Cu ions. It is presumed that Cu ions play a significant role in modulating the growth dynamics, resulting in the formation of bone nanorods with distinct structural characteristics. Conversely, when Pt foreign metal ions are employed in the growth process, this effect is not observed [25]. This comparison highlights the specific influence of Cu ions in dictating the growth behaviour of Au nanoseed leading to the formation of nanorods and bone nanorods.

To study the structural properties, the GBNRs sample that was prepared using 5 hours of growth time was chosen and evaluated using XRD characterization as shown in Figure 6. It can be seen from the figure that all diffraction peaks attributed to GBNRs corresponded to the face-centered cubic (FCC) structure of gold according to the standard data for gold (ICSD file No. 98-061-1623). Lattice spacing computed from the strongest diffraction peak, plane (111), is 0.235 nm, which matches well with the HR-TEM result. Moreover, the EDS spectrum as shown in Figure 7 reveals that the elemental composition of the bone nanorods is Au atoms. As previously mentioned, Cu is not formed in the end product and this is confirmed by the Cu peak that does not appear in the XRD spectrum.

To thoroughly understand the growth mechanism of GBNRs, we conducted a detailed analysis of the nanoparticles' morphology that form during the seed and growth processes. Initially, the nucleation and growth of these nanoparticles commence from Au nanoseeds, which exhibit {110}, {111}, and {100} crystal facets [26]. It is noteworthy that the under potential deposition (UPD) of the {110} facet is higher than the {100} and {111} facets, leading to the preferential adsorption of a CTAB bilayer on the {110} facet [27].

During the growth process, Ag ions derived from $AgNO_3$ which are added in growth solution, react with bromide ions originating from the CTAB surfactant, resulting in the formation of AgBr. Remarkably, AgBr selectively adsorbs onto the {110} facets [28], thereby influencing the subsequent deposition of Au atoms. Due to the higher surface energy of the {110} facet, Au atoms predominantly deposit onto {100} and {111} facets rather than {110} facets, as greater surface energy implies less stability [29].

As the reaction time increases, the quantity of Cu ions as foreign metal which deposited onto the {100} facets increase. Since Cu has the higher reactivity compared to Au, Cu atoms accumulate on the {100} facet facilitating the adsorption of Br to form CuBr on this facet. Consequently, the growth rate on the {100} facet is suppressed. Meanwhile, the deposition of Au atoms persists on the {111} facets. Ultimately, this intricate process leads to the formation of GBNRs.
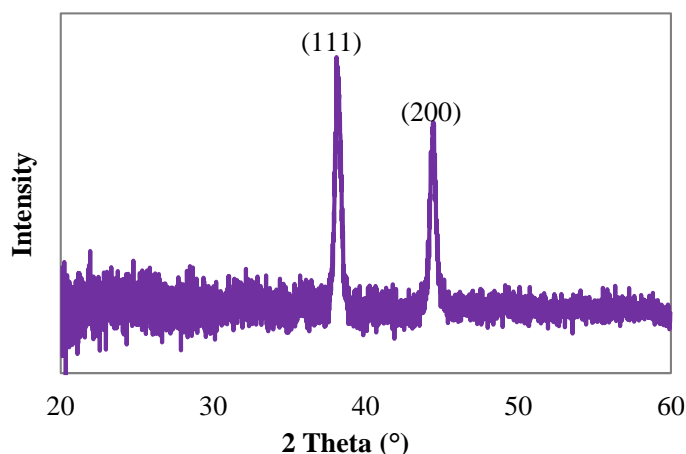

Figure 6. XRD pattern of GBNRs obtained at growth time 5 hours
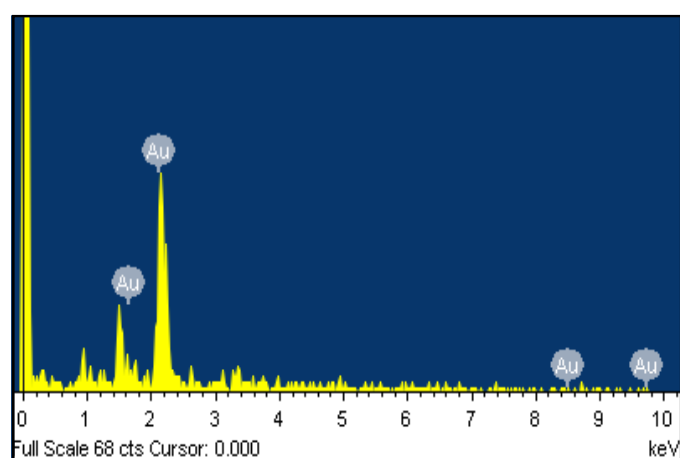

Figure 7. EDS spectrum of GBNRs obtained at growth time 5 hours

It is important to note that this mechanism does not occur if the foreign metal ion in the growth solution is substituted with an atom other than Cu (e.g., Pt atom), as previously reported in our work [30]. For further clarity, the illustration of the GBNRs growth mechanism is shown in Figure 8.

4. CONCLUSION

In conclusion, the introduction of copper replacing platinum as the foreign metal ion successfully produced GBNRs. The synthesis of GBNRs was accomplished through the SMGM, employing two distinct stages: the seeding and growth processes. In this research, GBNRs were synthesized for two hours for the seeding process and variation of the growth process time. It was found that the optimum growth time is 5 hours. The GBNRs have two resonance peaks for t-SPR and l-SPR at 583 nm and 766 nm for the 5 hours of growth time with an aspect ratio of 2.46 ± 0.06 and surface density of 64.92 %. HR-TEM images reveal that bone nanorods are formed from rods with reduced overgrowth rate in the [100] direction for the tips regions and in the [110] direction for the edges regions. The reduced overgrowth is presumably from the effect of Cu ions as the effect is not observed when Pt foreign metal ions are employed for the growth process.
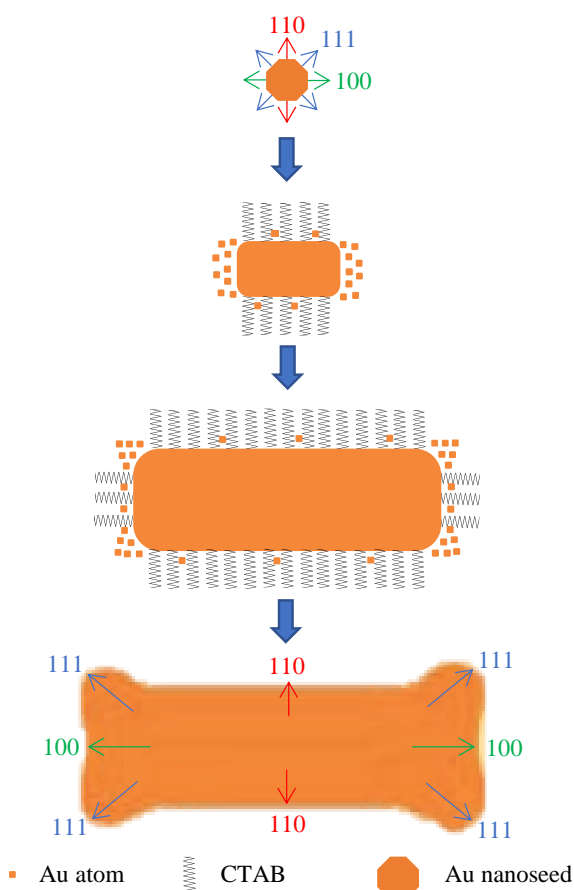
Figure 8. Schematic illustration of the growth mechanism of GBNRs

Based on the morphology of the nanoparticles formed, the possible growth mechanism of GBNRs is as follows: the initial nucleation and growth of nanoparticles come from Au nanoseeds which have {110}, {111}, and {100} crystal facets. Since the surface energy of the {110} facet is higher than {100} and {111} facets, the CTAB bilayer is adsorbed on the {110} facet. The Ag ions from $AgNO_3$ in the growth solution react with bromide ions from CTAB surfactant and form AgBr, which selectively adsorb onto {110} facets. Consequently, the Au atoms will predominantly deposit onto {100} and {111} facets instead of {110} facets because greater surface energy means less stability. As the reaction time increases, more Cu ions, which are foreign metal ions in the growth solution, will be deposited on the {100} facets. Since Cu is more reactive than Au, more Cu ions have been deposited on the {100} facets, facilitating the adsorption of Br to form CuBr on these facets, thus slowing the growth rate on {100} facets. On the other hand, the deposition of Au atoms on the {111} facets still occur. Ultimately, this process culminates in the formation of GBNRs.

ACKNOWLEDGMENTS

REFERENCES

[1] S. Her, D. A. Jaffray, and C. Allen, "Gold nanoparticles for applications in cancer radiotherapy: Mechanisms and recent advancements," *Advanced Drug Delivery Reviews*, vol. 109, pp. 84–101, 2017.

[2] S. Nafisah *et al.*, "One-step wet chemical synthesis of gold nanoplates on solid substrate using poly-l-lysine as a reducing agent," *MethodsX*, vol. 5, pp. 1618–1625, 2018.

[3] M. Salve, A. Mandal, K. Amreen, P. K. Pattnaik, and S. Goel, "Greenly synthesized silver nanoparticles for supercapacitor and electrochemical sensing applications in a 3D printed microfluidic platform," *Microchemical Journal*, vol. 157, p. 104973, 2020.

[4] P. Prosposito, L. Burratti, and I. Venditti, "Silver Nanoparticles as Colorimetric Sensors for Water Pollutants," *Chemosensors*, vol. 8, no. 2, p. 26, 2020.

[5] F. C. Barreto, M. K. L. da Silva, and I. Cesarino, "Copper Nanoparticles and Reduced Graphene Oxide as an Electrode Modifier for the Development of an Electrochemical Sensing Platform for Chloroquine Phosphate Determination," *Nanomaterials*, vol. 13, no. 9, p. 1436, 2023.

[6] L. Wang, M. Hasanzadeh Kafshgari, and M. Meunier, "Optical Properties and Applications of Plasmonic-Metal Nanoparticles," *Advanced Functional Materials*, vol. 30, no. 51, 2020.

[7] S. Nafisah *et al.*, "Improved Sensitivity and Selectivity of Direct Localized Surface Plasmon Resonance Sensor Using Gold Nanobipyramids for Glyphosate Detection," *IEEE Sensors Journal*, vol. 20, no. 5, pp. 2378–2389, 2020.

[8] M. Morsin, M. M. Salleh, M. Z. Sahdana, and F. Mahmud, "Investigation on the Growth Process of Gold Nanoplates Formed by Seed Mediated Growth Method," *Procedia Engineering*, vol. 184, pp. 637–642, 2017.

[9] C. J. Murphy *et al.*, "Gold nanorod crystal growth: From seed-mediated synthesis to nanoscale sculpting," *Current Opinion in Colloid & Interface Science*, vol. 16, no. 2, pp. 128–134, 2011.

[10] N. Z. An'Nisa, M. Morsin, R. Sanudin, N. L. Razali, S. Nafisah, and N. Bakar, "High Sensitivity Plasmonic Based on Triclopyr Butotyl Herbicide Sensor using Gold Nanorods (GNRs) as Sensing Material," *ASM Science Journal*, vol. 12, no. Special Issue 4, pp. 139–146, 2019.

[11] N. L. Razali *et al.*, "Formation of anisotropic gold nanoparticles on indium tin oxide substrates as a plasmonic sensing material," *Nanomaterials and Nanotechnology*, vol. 10, p. 184798042096538, 2020.

[12] N. Z. An'Nisa, M. Morsin, R. Sanudin, N. L. Razali, and S. Nafisah, "Controlled wet chemical synthesis of gold nanorods for triclopyr butotyl herbicide detection based-plasmonic sensor," *Sensing and Bio-Sensing Research*, vol. 29, p. 100359, 2020.

[13] M. Morsin, S. Nafisah, R. Sanudin, N. L. Razali, F. Mahmud, and C. F. Soon, "The role of positively charge poly-L-lysine in the formation of high yield gold nanoplates on the surface for plasmonic sensing application," *PLOS ONE*, vol. 16, no. 11, p. e0259730, 2021.

[14] M. Morsin, M. Mat Salleh, A. Ali Umar, and M. Sahdan, "Gold Nanoplates for a Localized Surface Plasmon Resonance-Based Boric Acid Sensor," *Sensors*, vol. 17, no. 5, p. 947, 2017.

[15] S. Nafisah *et al.*, "Growth time dependency on the formation of gold nanobipyramids for efficient detection towards chlorpyrifos-based LSPR sensor," *Optik*, vol. 289, p. 171270, 2023.

[16] S. Nafisah, M. Morsin, R. Sanudin, N. L. Razali, Z. M. Zain, and M. Djamal, "Gold Nanobipyramids as LPSR Sensing Materials for Glyphosate Detection: Surface Density and Aspect Ratio Effect," *IEEE Sensors Journal*, vol. 22, no. 19, pp. 18479–18485, 2022.

[17] N. Z. A. Md Shah, M. Morsin, R. Sanudin, N. L. Razali, S. Nafisah, and C. F. Soon, "Effects of Growth Solutions Ageing Time to the Formation of Gold Nanorods via Two-Step Approach for Plasmonic Applications," *Plasmonics*, vol. 15, no. 4, pp. 923–932, 2020.

[18] H. Chen, L. Shao, Q. Li, and J. Wang, "Gold nanorods and their plasmonic properties," *Chem. Soc. Rev.*, vol. 42, no. 7, pp. 2679–2724, 2013.

[19] S. Nafisah, M. Morsin, N. Nayan, N. A. Jumadi, N. L. Razali, and N. Z. A. M. Shah, "Synthesis of Gold Nanorices on ITO Substrate Using Silver Seed-Mediated Growth Method," *International Journal of Integrated Engineering*, vol. 9, no. 4, pp. 124–128, 2017.

[20] C. Fang, G. Zhao, Y. Xiao, J. Zhao, Z. Zhang, and B. Geng, "Facile Growth of High-Yield Gold Nanobipyramids Induced by Chloroplatinic Acid for High Refractive Index Sensing Properties," *Scientific Reports*, vol. 6, no. 1, p. 36706, 2016.

[21] S. Nafisah, Iwantono, M. Morsin, Y. Citra, S. Melani, and N. L. Razali, "Optical Properties of the Amine Functionalized Gold Nanobipyramids: Effect of Functionalization Times Period," *International Journal of Nanoelectronics and Materials*, vol. 13, no. 4, pp. 615–624, 2020.

[22] Iwantono *et al.*, "Application of Anisotropic Gold Nanomaterials in Plasmonic Sensors for Detection of Glyphosate," *Journal of Physics: Conference Series*, vol. 2672, no. 1, p. 012017, 2023.

[23] S. A. Lee and S. Link, "Chemical Interface Damping of Surface Plasmon Resonances," *Accounts of Chemical Research*, vol. 54, no. 8, pp. 1950–1960, 2021.

[24] N. Salsabiila, M. Morsin, S. Nafisah, N. L. Razali, F. Mahmud, and Z. Tukiran, "Mini Review of Glucose Detection Using Plasmonic Sensor," *Emerging Advances in Integrated Technology*, vol. 4, no. 1, 2023.

[25] N. Salsabiila, M. Morsin, M. H. Hasbullah, S. Nafisah, N. L. Razali, and Iwantono, "Thiol Functionalized Gold Nanobipyramids-Based Plasmonic Sensor For Glucose Detection," *IIUM Engineering Journal*, vol. 25, no. 1, pp. 274–290, 2024.

[26] G. González-Rubio *et al.*, "Revisiting the Role of Seed Size for the Synthesis of Highly Uniform Sub-10 nm Length Gold Nanorods," *Chemistry of Materials*, vol. 36, no. 4, pp. 1982–1997, 2024.

[27] M. Grzelczak, J. Pérez-Juste, P. Mulvaney, and L. M. Liz-Marzán, "Shape Control in Gold Nanoparticle Synthesis*," in *Colloidal Synthesis of Plasmonic Nanometals*, 1st ed., Jenny Stanford Publishing, 2020, p. 24.

[28] J. Zhu and R. B. Lennox, "Insight into the Role of Ag in the Seed-Mediated Growth of Gold Nanorods: Implications for Biomedical Applications," *ACS Applied Nano Materials*, vol. 4, no. 4, pp. 3790–3798, 2021.

[29] M. Brown and B. J. Wiley, "Bromide Causes Facet-Selective Atomic Addition in Gold Nanorod Syntheses," *Chemistry of Materials*, vol. 32, no. 15, pp. 6410–6415, 2020.

[30] S. Nafisah *et al.*, "Effect of additive acid on seeded growth of gold nanobipyramids," *Journal of Physics and Chemistry of Solids*, vol. 148, p. 109764, 2021.